

Performance of a Busbar Differential Protection Based on EMTP Simulation and Digital System Tests

by

Jules Esztergalyos
Bonneville Power Administration
Portland, OR

Dr. Joachim Bertsch
ABB Network Partner Ltd.
Schwitzerland

Majda Ilar
ABB Network Partner Ltd.
Switzerland

Presented before the
24th Annual
Western Protective Relay Conference
Spokane, Washington
October 20-23, 1997

Performance of a Busbar Differential Protection Based on EMTP Simulation and Digital System Tests

by

Jules Esztergalyos
Bonneville Power Administration
Portland, OR

Dr. Joachim Bertsch
ABB Network Partner Ltd.
Schwitzerland

Majda Ilar
ABB Network Partner Ltd.
Switzerland

Abstract - Modern software and digital real-time communication technology have made it possible to develop a fully numerical decentralized bus differential and breaker failure protection system.

To test the new algorithms developed for the bus differential protection EMTP based simulation and digital test methods are described.

The saturation of current transformers is probably the most critical issue also for digital bus differential protection. It affects the accurate measurement of the currents which is most important as parts of the protection algorithms. Solutions were worked out using new methods of digital signal processing.

The paper describes the modular software structure, the logical design and the theoretical fundamentals of the protection algorithms embedded in the flexible hardware of this digital bus differential protection system.

The effects of current transformer saturation were compensated on-line in the digital signal processor. Therefore the system will never block in case of heavy current transformer saturation. To test this functionality two different testing methods are described. The most work in development of the protection algorithms was done by off-line tests with simulations.

Modern simulation methods are shown which in combination with the use of digital relaying enable the verification of the entire protection algorithms in a very precise way.

The results of the computation of current wave forms in ComTrade file format testing the system with digital playback/on-line tests are presented.

Finally a summary of the results showing the high stability of a numerical bus differential protection system, even in cases where current transformers extremely saturate is given.

I. System Structure

New algorithms are used in a decentral, fully numerical busbar protection system is shown in Figure 1. [1], [2], [3].

Fully numerical signal processing is realized in this new system. Formerly, busbar protection systems used to be realized in analogue technique. In this new system the whole protection function is based on numerical algorithms. The protection system offers individual numerical evaluation of each phase and the zero-sequence system.

The execution of the algorithms are shared by the bay units and the central unit. Each bay unit continuously monitors the currents of the feeder to which it is assigned. Simultaneously it reduces the effects of current transformer saturation and performs the Fourier-filtering [4].

The data is transferred between the bay units and the central unit via optical fiber links. To transmit the information via optical links, a bus system connecting the bay units with the central unit is indispensable. A transmission capacity limit due to physical-technical reasons is unavoidable. Above all, the complex fundamental frequency current phasors of the busbar feeder currents $I_{L,n}$ of the phases $L \in \{R, S, T\}$ must be transmitted from the bay unit to the central unit. This is sufficient information to run two independent protection algorithms:

- a stabilized current differential algorithm and
- a comparison of current directions (phase comparison).

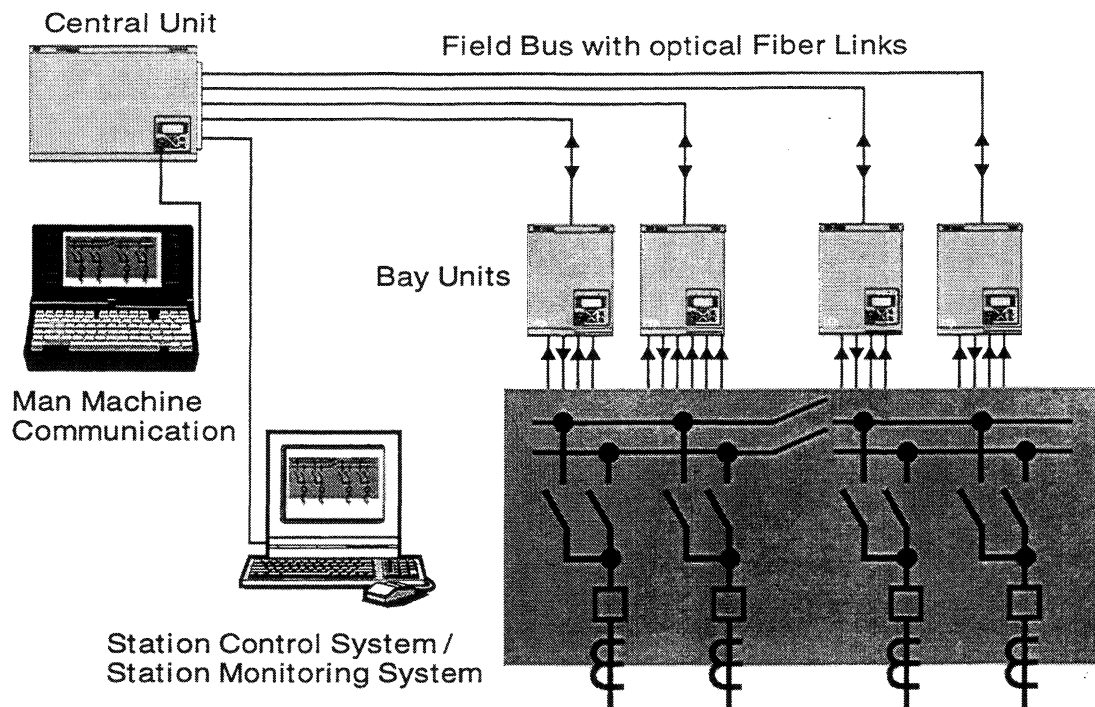


Figure 1. Decentralized Numerical Bus Protection System Diagram.

II. Protection Algorithms

A. Stabilized current differential algorithm

The stabilized differential current algorithm is based on the rule of Kirchhoff (sum of currents entering and leaving busbar must be equal zero all the time in the normal operation). Since the current transformers may be charged with strongly differing overcurrents, differential currents may occur erroneously due to uneven saturation effects. In this respect, the stabilized differential algorithm is basically advantageous.

The structure of the protection algorithm is shown in Figure 2. This algorithm is based on the current differential principle; it uses the restraint current for stabilization. The differential current is formed by the sum of all feeder currents. The differential currents I_{Diff} for each of the phases L amount to:

$$I_{Diff} = \left| \sum_{n=1}^N I_{Ln} \right| \quad (1)$$

and the restraint current I_{Rest} is calculated from

$$I_{Rest} = \sum_{n=1}^N |I_{Ln}| \quad (2)$$

where N is the number of feeders. The following two conditions have to be accomplished for the detection of an internal fault:

$$k_{st} = \frac{I_{Diff}}{I_{Rest}} > k_{st\ max} \quad (3)$$

$$I_{Diff} > I_{K\ min} \quad (4)$$

where

k_{st} is the stabilizing factor,

$k_{st\ max}$ is the limit of stabilization factor,

$k_{st\ max} = 0.85$ is a typical value and

$I_{K\ min}$ is the threshold for the differential current.

The calculations and evaluations described in this chapter is performed by the central unit.

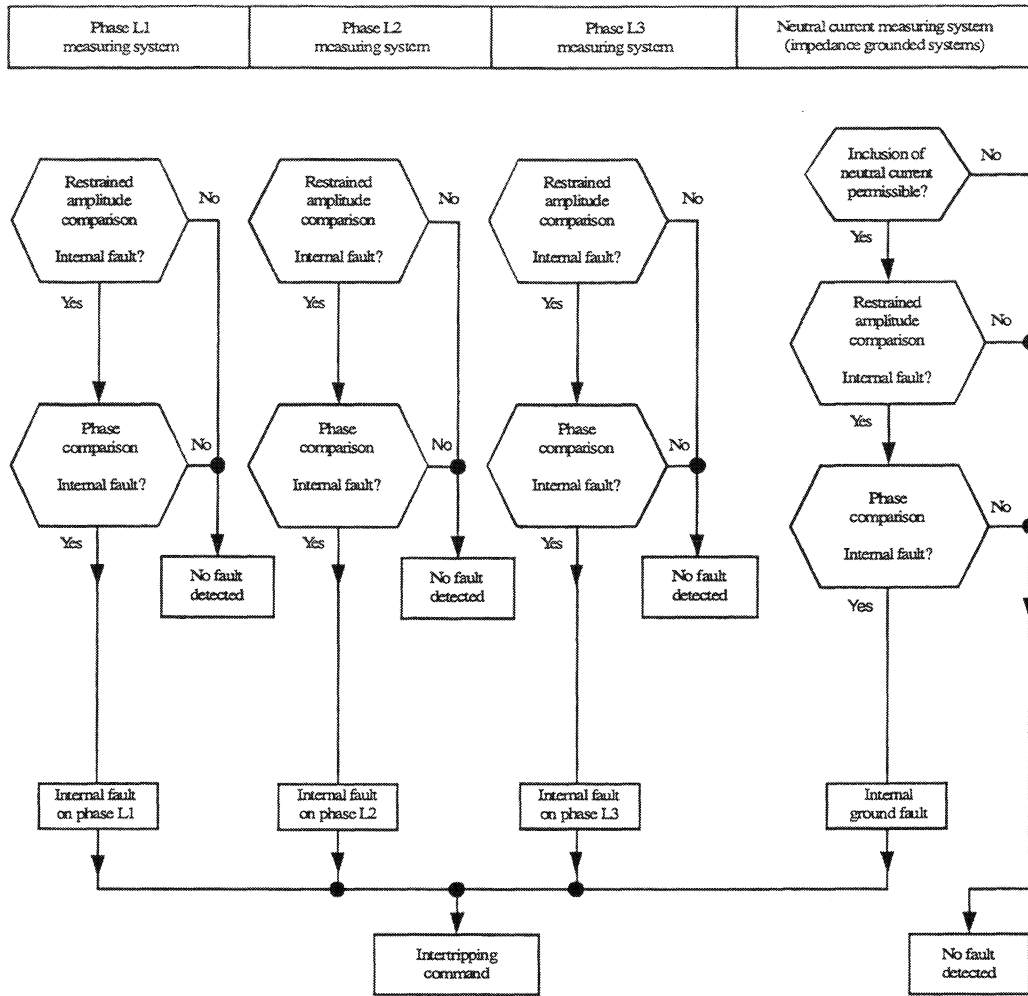


Figure 2. Structure of the Protection Algorithm

The tripping characteristic caused by (3) and (4) is shown in Figure 3.

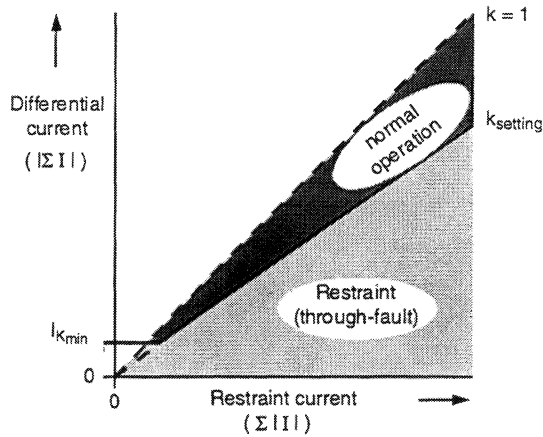


Figure 3. Tripping Characteristic of stabilized Current Differential Algorithm.

B. Phase Comparison Algorithm

The phasors of the fundamental frequencies current phasors $\varphi_{L,n}$ (5) are compared. In case of an internal fault, all of the feeder currents have almost equal phasors. If there are differences of about 180° between feeder currents, the system is either in normal operating mode or an external fault has occurred.

$$\varphi_n = \arctan \left[\frac{\text{Im}(I_{Ln})}{\text{Re}(I_{Ln})} \right] \quad (5)$$

If the minimal phase difference $\Delta\varphi$ between all combinations of phasors of the feeder currents is smaller than the tripping phasor for phase comparison $\Delta\varphi_{min}$ (6) the algorithm detects an internal fault shown in Figure 4.

$$\Delta\varphi < \Delta\varphi_{\min} \quad (6)$$

Empirically, $\Delta\varphi_{\min} = 74^\circ$ has proved to be a favorable threshold value for the tripping characteristic. The phase differences in cases 1 and 2 were caused by current transformer saturation or load current Fig.4.

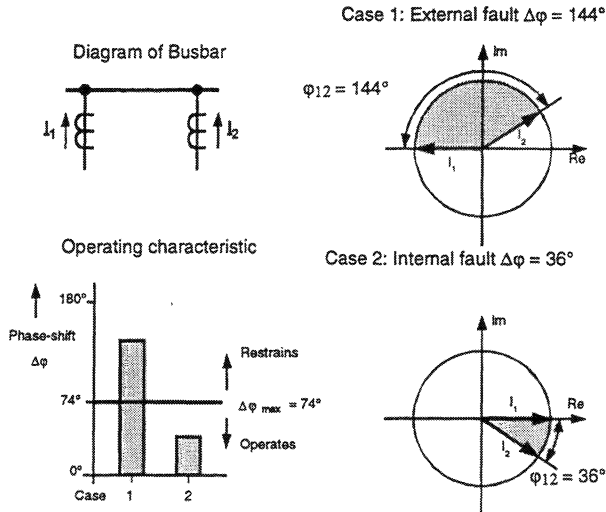


Figure 4. Phase Comparison Tripping and Blocking Characteristic.

In Figure 5 results using this principle are compared to those using with a reference phasor. Only phasors of feeders with a current magnitude over 0.8 times of the normal are valid for the comparison of current directions.

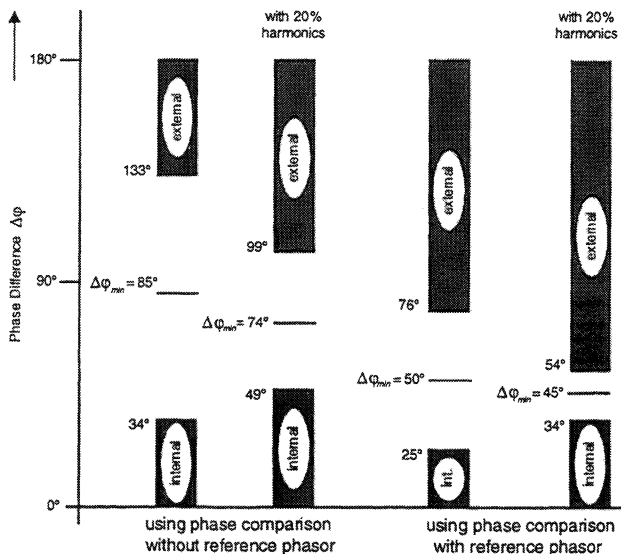


Figure 5. Phase Comparison: Simulation with Test Data.

Analog protection schemes were used to compare the phasors of the feeders to the phasor of the differential current, which was therefore the reference phasor [5]. In case of current transformer saturation, however, corresponding numerical phase comparison algorithms realizing numerical methods do not work optimally (Figure 5). The distinction between external and internal faults is not as pronounced as it is using phase comparison without a reference phasor.

Figure 5 results from simulations taking heavily saturated currents on a busbar with two feeders (Figure 4) into consideration. Besides, datasets with 20% harmonics (3rd, 5th, 7th or 9th order) of the amplitude of the fundamental frequency are used. The saturated current curves are also processed by the Maximumholding algorithm described in Chapter III. below.

C. Logic design

Only if both the stabilized current differential algorithm and the comparison of current directions algorithm detect an internal fault, the trip commands to the circuit breakers are given. Thus high security and selectivity are being accomplished.

III. CT Saturation

The busbar protection system is working correctly for external and internal faults also in case of current transformer saturation: The influence of current transformer saturation is compensated in each bay unit by a special method, which is applied prior to Fourier-filtering. This method is called Maximumholding and is presented explicitly in this chapter.

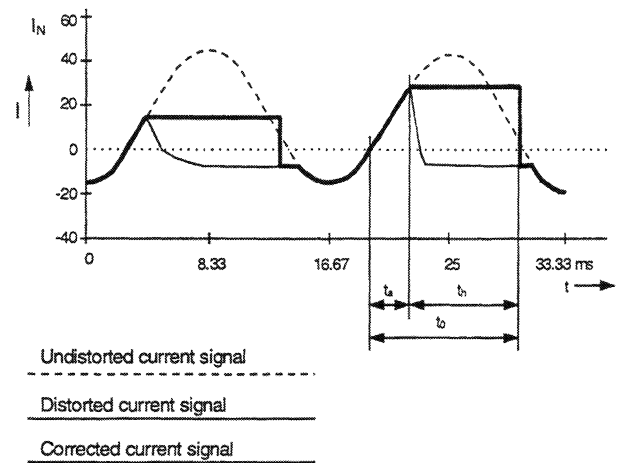


Figure 6. Maximumholding

The magnitude and phase of the fundamental-frequency signal with saturation obtained after Fourier-filtering shown in Figure 6 would be completely different from those obtained from the signal without saturation. Therefore the fundamental-frequency needs to be corrected in respect to phase and magnitude. Fourier-filtering of the signal corrected by Maximumholding provides a good approximation of the magnitude and phase of the fundamental frequency signal without saturation, so that this information can be used by the protection algorithms.

The basic function of the method of Maximumholding is to extract the maximum current magnitude I_{fmax} from the sample window (one power cycle) and to hold it for a defined holding time t_h . The current value will be held on the maximum value. The rise time t_a means the time interval between the latest zero crossing and the maximum value (Figure 6). Where t_h is:

$$t_h = t_o - t_a \quad (7)$$

Equation (7) shows that higher rise times t_a force shorter holding times t_h .

IV. Results of Simulations

The simulations are based on various sets of datas of internal and external faults and events on busbars including additional condition effects like current transformer saturation, harmonic distortion, transformer inrush and auto-reclosure. A special software tool has been developed to simulate the effects of saturation on all known types of current transformers [6]. Since the numerical current transformer model simulates the magnetic flux of the transformer core, it is capable of producing the secondary current curve belonging to any primary current curve.

A Δk_{st} - value (8) has been defined as the difference between minimum stabilizing factor $k_{st\ int}$ at internal fault and maximum stabilization factor $k_{st\ ext}$ at external fault, using the stabilized differential current algorithm.

$$\Delta k_{st} = \text{Min}(k_{st\ int}) - \text{Max}(k_{st\ ext}) \quad (8)$$

The Δk_{st} - value is a mean of measuring the capability of the algorithm to distinguish between internal and external faults. If the Δk_{st} - value becomes negative, no distinction can be made. In table I the results of characteristic testdata with different degrees of current transformer saturation, including heavy saturation, are shown.

Table I
Maximumholding: Results with Testdata

Method of Preprocessing	Δk_{st}	maximal k_{st} at external fault Max ($k_{st\ ext}$)	minimal k_{st} at internal fault Min ($k_{st\ int}$)
without Maximumholding	-0.12	0.91	0.79
Maximumholding	0.39	0.57	0.96

The results in table I are obtained from the simulations recorded in Figures 7 and 8. In these figures the results of all sample windows of each current testdata are marked by either an "o" or an "x". An "o" represents an external fault; an "x" represents an internal fault.

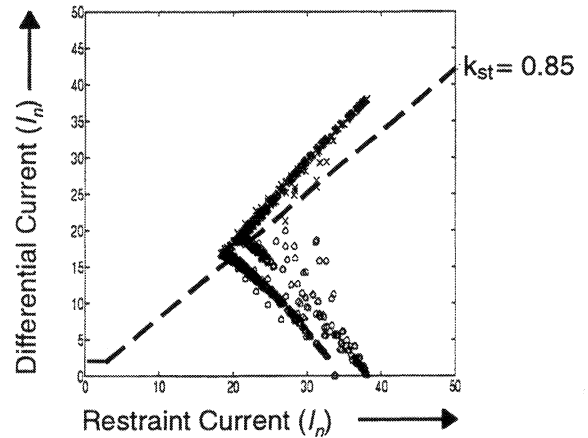


Figure 7. Results of Simulation without Maximumholding.

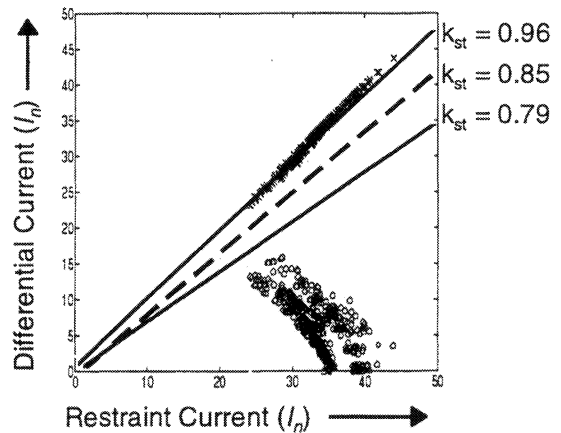


Figure 8. Results of Simulation with Maximumholding.

Comparing Figure 8 to Figure 7 it becomes obvious, that with the method of Maximumholding the distinction between internal and external faults can be made with sufficient security (Figure 8) in contrast to Figure 7, where no Maximumholding has been used.

For the phase comparison algorithm the method of Maximumholding is suited as well (Figure 4). As for Figure 7 and 8 this algorithm produces satisfactory results only by applying the method of Maximumholding.

The method of Maximumholding is started for currents higher than 2.5 times of the feeders normal current. The reset is controlled with an hysteresis of 70%. This indicates that the method of Maximumholding represents a powerful and secure applicable numeric tool for compensating effects of current transformer saturation on protection systems in general.

V. Field of Applications

A. General

The protection algorithms are suited for busbar protection systems also in solidly grounded power systems. The algorithms of chapter II work phase selectively.

B. Current-limiting grounded power systems

In order to reach a sufficient sensitivity for applying the busbar protection system in current-limiting grounded power systems, the zero-sequence current will be supervised. For this purpose, additional algorithms were developed. In this chapter, the new algorithms used for the zero-sequence current supervision as well as their integration in the protection system are described.

In current-limiting grounded systems phase-to-earth faults cannot be detected reliably using the stabilized differential current algorithm alone. The short-circuit-current level might be too small. A solution is to take into account zero-sequence currents additionally by monitoring them with the phase comparison algorithm. Equation (9) shows how the phase φ_{0n} of a zero-sequence current at feeder n is determined.

$$\varphi_{0n} = \arctan \left[\frac{\text{Im}(I_{Rn}) + \text{Im}(I_{Sn}) + \text{Im}(I_{Tn})}{\text{Re}(I_{Rn}) + \text{Re}(I_{Sn}) + \text{Re}(I_{Tn})} \right] \quad (9)$$

If differential currents caused by current transformer inaccuracy can be excluded, monitoring the zero-sequence currents with the phase comparison algorithm guarantees the protection system's correct function. Current transformer saturation can be characterized by the share of certain harmonics contained in the zero-sequence current.

In case the zero-sequence current's harmonics content k_h is higher than the limit of the harmonic supervision $k_{h \max}$, the monitoring of the zero-sequence currents can be blocked (10).

$$k_h = \frac{|I_{02}| + |I_{04}| + |I_{06}|}{|I_{01}|} < k_{h \max} \quad (10)$$

where

$|I_{01}|$ is the magnitude of the fundamental frequency and $|I_{0n}|$ is the magnitude of the n th harmonic.

In numerous simulations of different busbar installations, $k_{h \max} = 0.3$ has been found to be a reasonable threshold value for the harmonic supervision. Still, if more than one phase is involved in a fault, only the principles and methods stated in chapter II must be applied. Thus, the zero-sequence current monitoring is blocked for faults involving more than one phase.

VI. EMTF Simulations

A. ATP, EMTF Simulation Programs

The Alternative Transients Program (ATP) is the most widely used version of the Electromagnetic Transients program (EMTF) in the world today. In no small part, the acceptance of ATP is due to its availability to nearly everyone in the world free of royalty, and its compatibility with the computers of most common interest. EMTF was developed in the public domain at the Bonneville Power Administration (BPA).

The test cases have been computed with ATP according to the single phase diagram shown in Figure 9. The simulation configuration consists of a 230kV bus with three sources connected via transmission lines to it and a simple load. The bus and the sources/loads are placed between circuit-breakers. The simulated configuration is based on a real existing busbar.

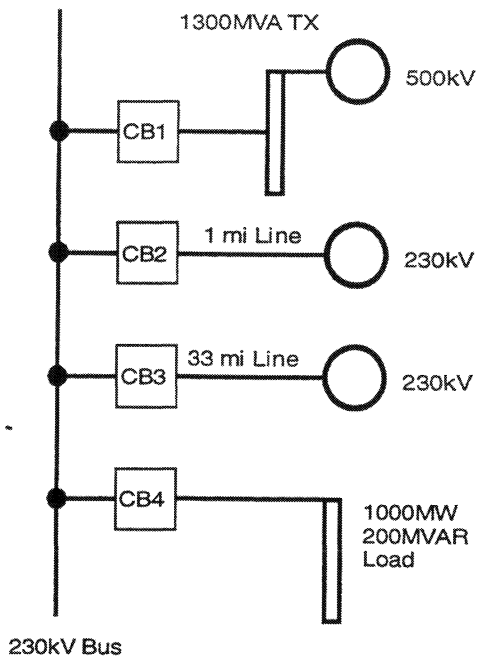


Figure 9. ATP Studies One Line Diagram

Different fault configurations are shown in table II. Four internal faults with various fault resistance and four external faults occurring at the four different circuit-breakers (with 0 Ohms fault resistance) are simulated as phase-A-to-ground faults. A sample data set of one A-phase feeder with heavy current transformer saturation is shown in Figure 10.

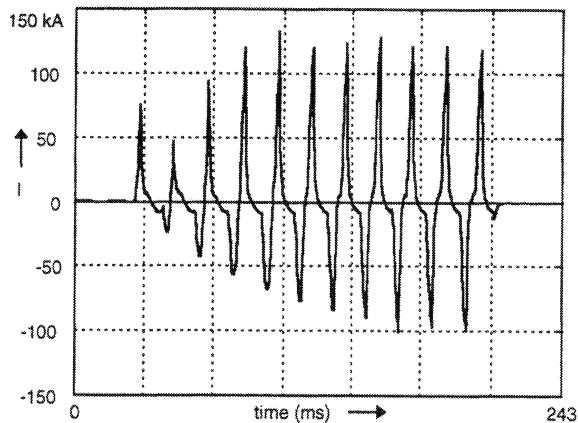


Figure 10. Test Wave with Saturation

The data sets, converted to ComTrade file format, are used in a combined software/hardware test system. Figure 11 gives an overview of the test system.

Simulation Control System

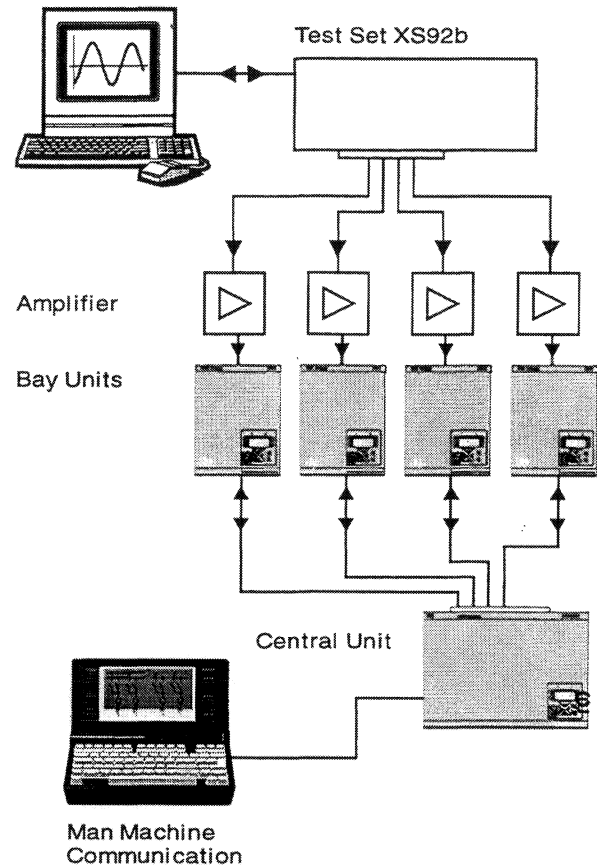


Figure 11. Hardware Components

The test values are written in the memory of the simulation control system and are transferred real-time to the XS92b test set. Here, the analog values are driven forward to four current amplifiers, one amplifier per bay unit. Each amplifiers drives four currents (3 phases and the zero-sequence current).

Reaction of the protection system is protocolled by an LaptopPC, connected via an optical fiber link to the protection system. On the PC, a MMI software is running for setting and controlling the busbar differential protection system.

Table II
ATP Simulation: Results

Test Case	Fault Location	Operate/Restraining	Short-circuit current	Operating time
1	A-ph Internal (R=0 ohms)	Operate	102 kAmps	26
2	A-ph Internal (R=4 ohms)	Operate	24 kAmps	35.9
3	A-ph Internal (R=10 ohms)	Operate	12 kAmps	45.1
4	A-ph Internal (R= 20 ohms)	Operate	6.5 kAmps	46.5
5	A-B-C External	Restraining	70 kAmps	-
6	A-B-C External	Restraining	42 kAmps	-
7	A-B-C External	Restraining	7 kAmps	-
8	A-B-C External	Restraining	102 kAmps	-

B. Results

Settings:

Threshold for the differential current $I_{K\ min}$ (equation (4)): 2000 A (R, S, T and 0 phase)

Stabilizing factor k_{st} (equation (3)): 0.8 (R, S, T, 0 phase)

With the test data containing internal faults the operation of the tested busbar differential protection system was correct and all faults were cleared successfully. The operating time in table II represents the complete minimum tripping time measured on the occasion of the simulations.

It has to be pointed out that the tripping of a very high resistive fault was successful with the tested busbar differential protection system (table II, test-case 4).

In recording external faults the protection behavior is stable (restrain) in every case, even at extreme current transformer saturation (table II, test-case 5, 6, 7 and 8).

VII. Conclusion

The authors presented a new algorithm, implemented in a new numerical busbar protection system. In general two separate, independent algorithms are used for each protected busbar zone and each phase. In installations with current-limiting (resistive) grounded networks the zero-sequence current is monitored additionally with a phase comparison algorithm including a harmonic supervision.

The method of Maximumholding provides the possibility to drastically reduce the performance requirements for current transformers. The algorithms are very robust against effects of saturation of the current transformers. This allows the busbar protection system to guarantee highest through-fault stability in spite of current transformer saturation. Due to continuous self-monitoring diagnosis, the high availability, dependability and security of the busbar differential protection is guaranteed by ATP simulations also proven.

VIII. References

- [1] D. M. Peck, B. Nygaard, K. Wadelius, "A New Numerical Busbar Protection System with Bay-Orientated Structure," in *Proceedings of the 1993 IEE Developments in Power System Protection Conference*.
- [2] U. Braun, *Konzepte und Algorithmen für den numerischen Sammelschienenschutz*; Dissertation am Institut für Energieübertragung und Hochspannungstechnik der Universität Stuttgart, 1994.
- [3] K. Feser, U. Braun, F. Engler, A. Maier "Application of Neuronal Networks in Numerical Busbar Protection Systems," in *Proceedings of the 1991 Application of neuronal Networks to Power Systems Conference*.
- [4] A.G. Phadke, M. Ibrahim and T. Hlibka, "Fundamental basis for distance relaying with symmetrical components," *IEEE Trans. on Power Apparatus and Systems*, vol. 96, no. 3, 1977, pp. 635-640.
- [5] H. Ungrad, G. Winkler, *Schutztechnik in Elektroenergiesystemen*, Berlin: Springer, 1991, pp 194-198.
- [6] J. Bertsch, W. Fromm, F. Oechsle "Stromwandler-Simulation unter Berücksichtigung von Hysterese," *Elektrotechnische Zeitschrift (ETZ)*, vol. 115, no. 19, October 1994, pp. 1108-1114.